

Flood type drives river-scale plastic deposition

Louise J. Schreyers,^{*,†} Rahel Hauk,[†] Nicholas Wallerstein,[†] Adriaan J. Teuling,[†]
Remko Uijlenhoet,^{†,‡} Martine van der Ploeg,[†] and Tim H.M. van Emmerik[†]

[†]*Hydrology and Environmental Hydraulics Group, Wageningen University, Wageningen*

[‡]*Department of Water Management, Delft University of Technology, Delft*

E-mail: l.schreyers@gmail.com

This manuscript is a non-peer reviewed preprint submitted to EarthArXiv. The manuscript has been submitted for peer review to the journal Environmental Science & Technology.

Abstract

Plastic pollution is considered a global environmental challenge, prompting international regulation efforts such as the UN plastic treaty to end plastic pollution. River basins, with high population densities and poor waste management, are particularly exposed to plastic pollution. Floods amplify plastic presence in rivers by mobilizing previously deposited and introduce new plastics. Yet, the fate of these mobilized plastics remains unclear, with observations suggesting either downstream export or floodplain deposition. This study assesses flood impact on plastic deposition along river floodplains, using data from fifteen events — five floods and ten non-flood conditions — across two Dutch rivers. Non-flood conditions were defined as events with return periods below bankfull discharge, while floods exceeded this threshold (1.5-year return period). Higher flood return periods increased plastic deposition, with the two largest floods depositing two to three times more plastic than non-flood conditions. Deposition mechanisms varied by flood type. Obstruction-based deposition dominated during

an extreme summer flood (summer 2021 in the Meuse), when plastics mainly accumulated in inundated vegetation. Low-energy deposition prevailed during a long winter flood (winter 2024 in the IJssel), with high plastic concentrations found in wide floodplain sections where flow velocities decreased. Floodplain characteristics, hydrological conditions and proximity to plastic sources drive the plastic depositional patterns on floodplains. Flood severity and plastic entry into the environment are both projected to increase. We therefore expect an even more prominent role of floods in the global distribution of plastic pollution.

Introduction

Plastic pollution is recognized as a global societal concern posing human health risks and worldwide ecosystem contamination¹. Despite its urgency, efforts to establish a legally binding global plastic treaty by the end of 2024 were unsuccessful², highlighting the ongoing challenges in achieving international consensus on plastic pollution mitigation. Rivers are particularly exposed to plastic waste leakage due to their connectivity to urban areas³, which are the primary entry points of plastic pollution⁴. In some cases, rivers have been found to contain plastic concentrations exceeding those in marine and coastal ecosystems⁵. Within river systems, riverbanks and floodplains are considered to be some of the largest sinks for plastic pollution, potentially storing more plastics than the river surface, water column, or riverbed sediments^{6,7}. The mechanisms driving plastic deposition on floodplains remain unresolved, although recent work points to the potential role of floods⁸⁻¹⁰, similar to that found with inorganic sediment and large wood^{11,12}.

Floods can cause significant damage to urban areas, leading to the influx of plastic waste and non-waste plastic items¹³. Flooding of non-urbanized floodplains can also mobilize plastic deposited during previous high-flow events. In addition to increased plastic transport, overbank flows can result in substantial plastic deposition onto the floodplains. To date, flood-driven plastic deposition and transport have only been documented for individual flood

events, such as the summer 2021 flood along the Meuse river^{9,14}, the winter 2015-16 flood in Northwest England⁵ and the winter 2018 flood in the Seine river in France¹⁵. While these studies provide valuable insights into plastic mobilization and deposition, they do not fully address the variability of deposition across different flood events or the role of river and floodplain characteristics in shaping these processes. A comprehensive understanding of how different flood types influence river-scale plastic deposition is missing. Flood characteristics such as type (fluvial, pluvial, coastal, and flash floods), duration, and magnitude can drive diverse transport mechanisms¹⁶. Additionally, the factors governing the spatial distribution of plastic deposition along floodplains remain largely unexplored, highlighting a critical gap in our understanding of river plastic dynamics.

In this paper, we investigated plastic deposition after fifteen events, including five floods, between 2018 and 2024, in the Rhine-Meuse delta. We quantified riverbank plastic concentrations under both non-flood and flood conditions, with flood conditions also including floodplain plastic concentrations. Non-flood hydrological conditions were defined as events with return periods below the threshold for bankfull flow, while floods were classified as events exceeding this threshold (1.5-year return period)^{17,18}. Specifically, we estimated riverbank plastic concentrations following five floods of varying magnitudes, from a two-year flood return period to a centennial flood, as well as during ten non-flood periods. The research focussed on two major lowland rivers in the Netherlands: the Meuse and the IJssel (a branch of the Rhine). In addition, we attributed plastic concentrations to the main drivers of plastic deposition, using a parsimonious modeling approach. Our approach is applicable to rivers and events beyond those analyzed in this paper. We considered ten factors, including river and floodplain characteristics, and proximity to potential plastic sources. Similar to sediment and large wood deposition, the longitudinal distribution of plastic along floodplains is likely influenced by the balance between supply and deposition factors, which determines floodplain capacity in storing plastics¹⁹. The factors driving deposition are related to river and floodplain morphology, vegetation coverage, and hydrodynamic conditions. These factors

were selected based on insights from research on plastic, sediment, and large wood deposition²⁰⁻²⁶. Using our modeling approach, we evaluated the degree to which each predictive factor explained the observed deposition patterns, providing new insights into the role of floodplains in retaining plastics during flood events.

Methods

Floodplain plastic observations

Plastic concentrations on Dutch floodplains are monitored biannually by volunteers from the *Schone Rivieren* (English: Clean Rivers) program²⁷. The sampled length, parallel to the waterline, is set at 100 meters. The sampling width is defined by visible debris left from recent high water events and extends up to 25 meters from the waterline. All visible litter items (>5 mm) are collected, counted, and categorized using the River-OSPAR classification²⁷. While the data includes all anthropogenic macrolitter, 94% of the items are plastic, so we refer to them as "plastic" in this study.

We used *Schone Rivieren* data for low-magnitude floods (winter 2020 and winter 2021) and non-flood conditions. For the summer 2021 Meuse flood, we used the data from Hauk et al.⁹. Additionally, we conducted field sampling along the IJssel in January and February 2024, following a similar protocol. The dimensions of the sampled areas for these two flood events were flexible, with often shorter lengths but larger widths. Over the course of ten days of fieldwork, a total of 23 sites were sampled along the IJssel river. Sampling involved counting and categorizing all visible plastics found on grass, within vegetation features (e.g., shrubs, bushes, reeds, trees), and along debris lines.

Mass concentrations were estimated by converting item counts to mass, using mean mass statistics from De Lange et al.²⁸. Plastic storage was estimated by multiplying concentrations by floodplain areas (cf. section ‘Plastic concentrations forecasting model’). The uncertainties in storage and concentration estimates are related to measurement and item-to-mass

conversion uncertainties. Quantifying observer bias in plastic sampling remains challenging due to their discrete nature, despite efforts²⁹. The time-equivalent [y] values in Table 1 represent the estimated duration required for plastic stored in the floodplains to be flushed out of the system, assuming annual plastic transport rates of 15–41 tons/y for the IJssel and 56–75 tons/y for the Meuse. These transport rates are based on observed floating plastic transport from³⁰ and were adjusted to total river transport by accounting for the fact that approximately 70% of the total transported plastic mass remains at the river surface, as reported by⁷.

Flood severity calculation

We considered five flood events: three on the Meuse and two on the IJssel (Table 1). River discharge data from the Netherlands Directorate-General for Public Works and Water Management³¹ was used to estimate flood return periods with the Gumbel probability distribution³² and annual discharge maxima. Discharge data from the Olst gauging station was used for the IJssel, while data from the Sint-Pieter station was used for the Meuse. Flood duration was defined as the period during which discharge exceeded the 1.5-year return period (Figure 1), approximating the bankfull discharge level in natural rivers^{17,18}. For non-flood conditions ($T < 1$), we applied a threshold-based approach, fitting a Generalized Pareto Distribution (GPD) for more accurate return periods estimates for moderate flow events³³.

Table 1: Flood event characteristics. ‘Summer’ and ‘winter’ are used for brevity to indicate the general season of the flood events. Note that events can span multiple months; for example, ‘winter 2024’ refers to the event that occurred in December 2023–January 2024.

River	Flood event	Maximum river discharge [m ³ /s]	Flood duration [d]	Flood return period [y]	Time since previous 1.5-year flood [d]
Meuse	summer 2021	3310	3.3	111	147
	winter 2021	1775	3.3	2.8	264
	winter 2020	1742	4.8	2.6	229
IJssel	winter 2024	1097	30.0	2.9	830
	winter 2021	804	10.0	1.9	266

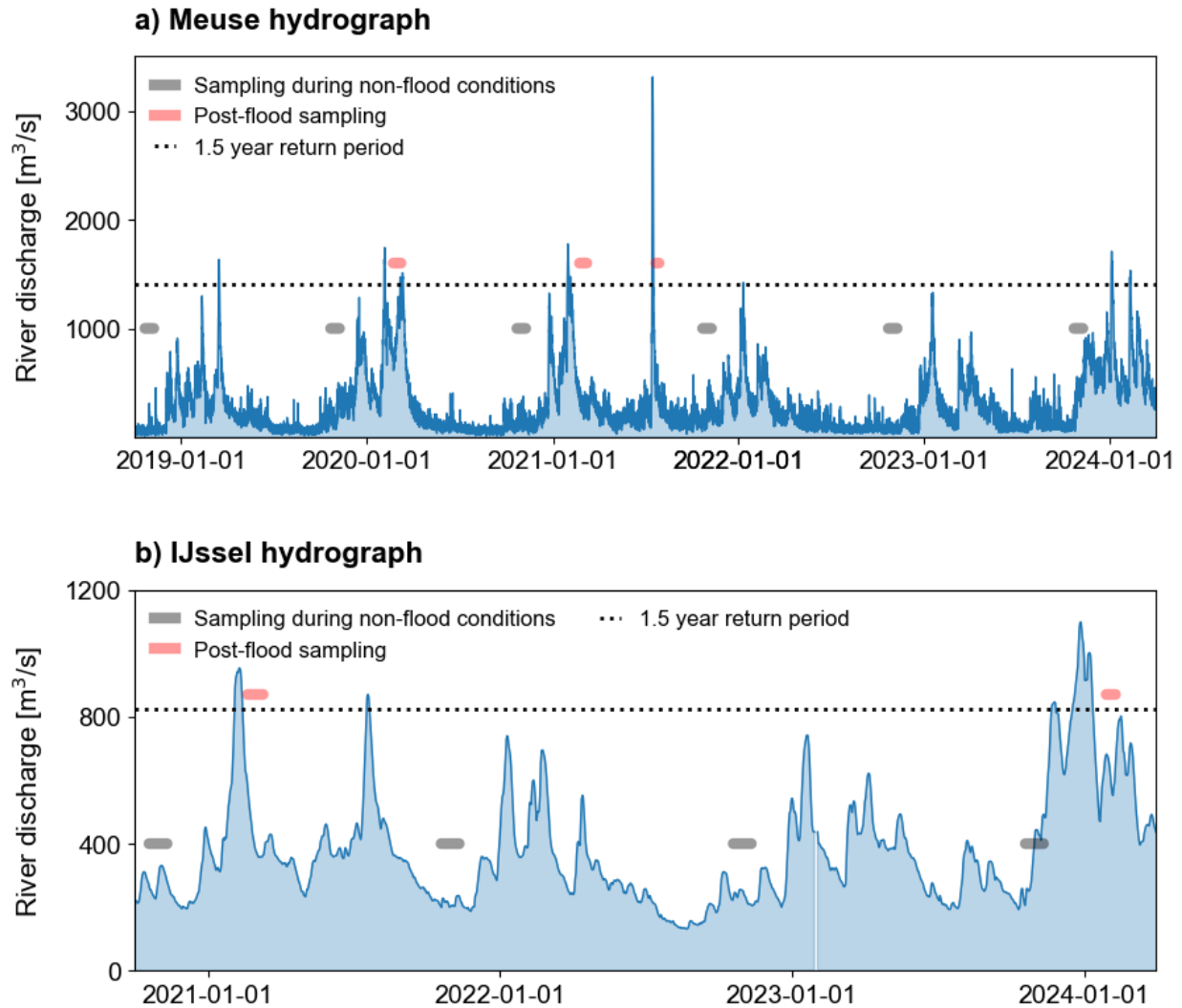


Figure 1: Hydrographs for plastic sampling during flood and non-flood conditions for the Meuse (a) and the IJssel (b). The variations in height for the sampling periods are only for illustrative purposes.

For the two higher-magnitude floods, flood severity was assessed along the river course (Figure 5). For the Meuse summer 2021 event, severity was estimated from multiple gauging stations³⁴, showing flood attenuation downstream. For the IJssel winter 2024 event, we estimated flood severity at Olst (the only discharge gauging station located along the IJssel, at km 68). For the upstream IJssel, flood severity was estimated based on discharge levels from the Lobith station (51.8619° N, 6.1186° E), using flow partitioning rates³⁵ to distribute flow across the Waal, Nederrijn, and IJssel. Estimates of flood severity based on Lobith and

Olst data both indicate a ~ 3 -year return period, showing minimal variation in flood severity along the IJssel.

Plastic concentrations forecasting model

Model description

We developed a general modeling framework, applicable to specific flood events and river systems, using event-specific Generalized Additive Models (GAMs)³⁶. The model includes ten factors - independent of hydrological conditions - categorized into three groups: i) floodplain characteristics (floodplain width, vegetation height, vegetation coverage index, lateral floodplain slope); ii) river course characteristics (sinuosity index, river channel width, river channel slope), and iii) proximity to potential sources (distance from upstream end of study area, distance from upstream Wastewater Treatment Plant, distance from upstream tributary) (Figure 2). These factors, selected based on literature, are expected to influence plastic deposition. Table 2 details each factor's expected effect. Some factors may have non-uniform effects, with positive or negative impacts depending on conditions such as flow rates, morphology, and floodplain characteristics.

Floodplain characteristics were extracted by dividing the floodplain into 100-meter sections along the river. The width of each section was determined using the floodplain boundaries defined by the Ecotopen dataset⁴². Vegetation height was estimated by subtracting Digital Surface Model (DSM) values from Digital Elevation Model (DEM) values^{43,44}. The vegetation coverage index was calculated using the Ecotopen vegetation classification. The floodplain lateral slope was also derived from the DSM. Since these three variables had two dimensions, we averaged the values for each 100-meter section to ensure consistency with the other variables. The river channel width was also determined for each 100-meter section. Other variables were selected at different resolutions. Sinuosity index was estimated over 2-km segments to balance resolution and prevent the sinuosity index from converging towards unity, which can occur when calculated over very short segments. The river channel slope

Table 2: List of variables anticipated to influence plastic deposition on floodplains, based on available literature on plastic, sediment and large wood deposition in river systems. Each variable is accompanied by hypotheses indicating the expected direction of the relationship: an upward arrow denotes that an increase in the variable correlates with greater plastic deposition, while a downward arrow indicates the opposite effect. Additional substantiation regarding the mechanisms of plastic deposition on floodplains is also provided.

Variable	Hypothesized response in deposition	Substantiation
Floodplain width	↑	Wider floodplains reduce cross-section averaged flow velocities ³⁷ , which in turn allows for greater deposition of plastic as the reduced energy of the water limits transport ³⁸ .
Floodplain vegetation height	↑	When the top vegetation height is lower than the inundation height, the vegetation acts as a physical barrier, trapping plastic and promoting deposition ²¹ .
	↓	When the vegetation height exceeds the inundation height, especially if only tree trunks are exposed to the flow, plastic items may bypass these features leading to reduced deposition or no noticeable effect.
Floodplain vegetation coverage	↑	Greater vegetation coverage increases terrain roughness, which promotes the deposition of plastic ²⁴ .
Floodplain lateral slope	↓	Gentle slopes may reduce the velocity of overbank flows, promoting the settling of plastic, while steeper slopes could maintain higher flow velocities, reducing deposition.
River channel sinuosity	↑	Larger sinuosity in the river's channel increases water turbulence and mixing, which can lead to higher and lower flow velocities around the bends, favouring the settling and accumulation of plastic on adjacent floodplains ²³ .
River channel width	↓	Narrower channels are more likely to result in trapping of plastic on bank side obstructions as compared with wider channels carrying the same discharge ³⁹ .
River channel slope	↓	Increased river channel slope, indicative of stream power, increases the transport capacity of rivers ²⁰ .
Distance from upstream end of study area	↓	Gradual reduction in transport load as plastics move downstream, particularly if potential plastic sources are located upstream of the study domain.
	↑	Proximity to river mouth can enhance plastic deposition, due to tidal dynamics ^(26,40) .
Distance from upstream WWTP	↓	WWTPs are point sources for plastic inputs into rivers ²² .
Distance from upstream tributary	↓	Tributary inflow can lead to an increase in plastic concentrations in rivers, increasing the availability of plastics for deposition ⁴¹ .
	↑	A clean tributary would actually dilute the plastic load of the main channel.

was calculated as the gradient of water surface elevation (dws) over longitudinal distance (dx) (Figure 2). The water surface elevation was derived from water level measurements at gauging stations³¹. The largest tributaries were manually selected, and the Waste Water Treatment Plant (WWTP) locations were extracted from *Stichting Nederlandse WaterSector*⁴⁵. All variables, except in data-poor sections between km 68 and 82 of the Dutch Meuse (Figure S2a in Supporting Information), were documented for each section.

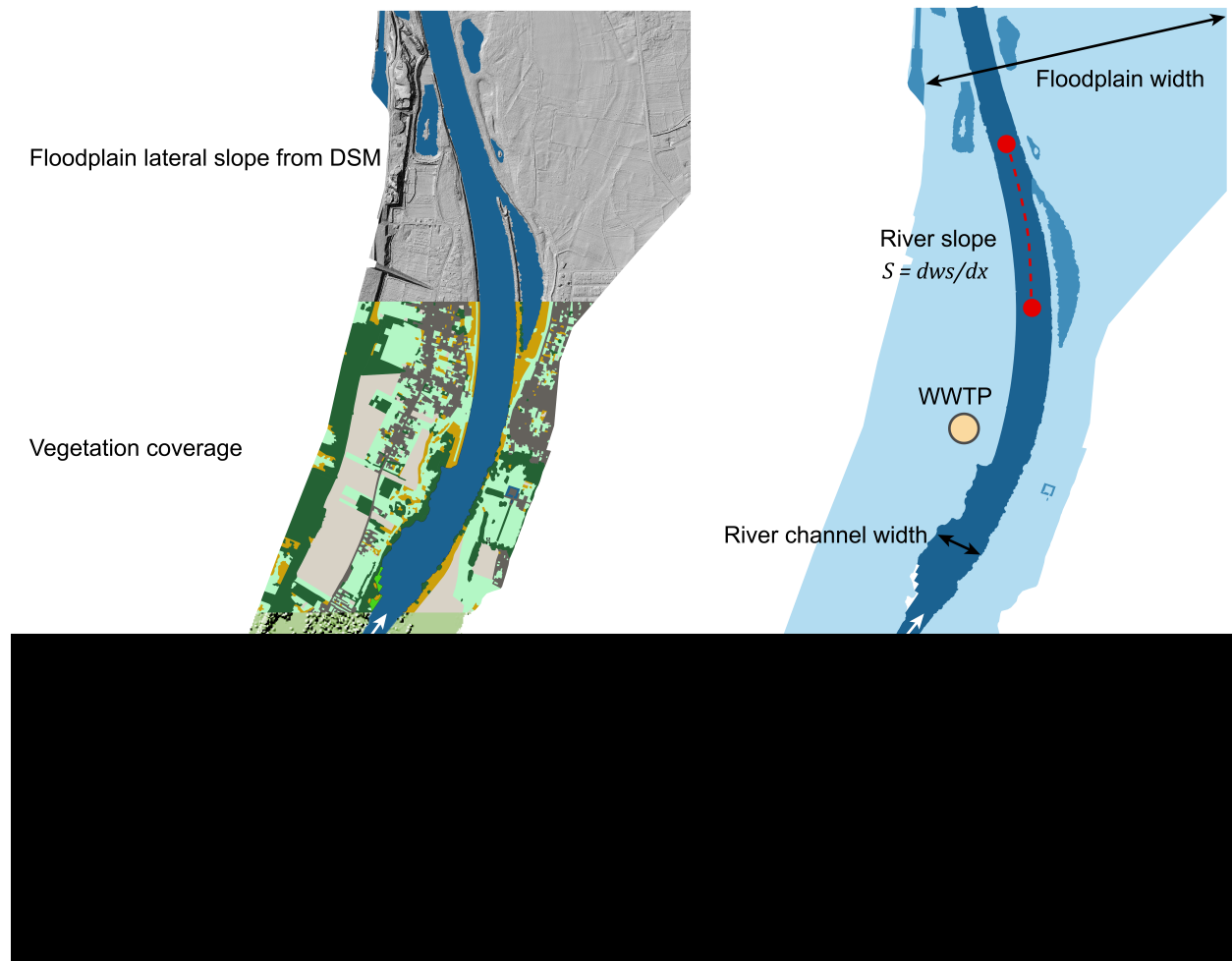


Figure 2: Schematic representation of the ten factors included in the model framework for simulating plastic concentrations. Note that specific model formulations often do not include all ten factors. The area represent the river channel and its floodplains. Here, dws represents the difference in water surface elevation, and dx represents the horizontal distance separating those two points.

Model performance

The models were initially fitted with all ten variables as linear terms. To improve model performance, we adjusted the formulation by excluding variables with limited explanatory power. We also fitted some variables as exponential terms after exploring the Spearman’s ρ values (not shown). This iterative process allowed for optimization by balancing the complexity and performance of the model. Model performance was evaluated using the R^2 and the Akaike Information Criterion (AIC) values, where a lower AIC indicated better performance for models with similar R^2 values. Table S1 (Supporting Information) details the various model formulations, with overall model performance and coefficients for each variable. For the Meuse summer 2021 event, model formulation ‘1.c’ was chosen as the best fitting model, while for the IJssel winter 2024 event, model formulation ‘10.c’ was selected.

To assess model robustness, we conducted a bootstrap analysis⁴⁶, using a ‘leave-one-out’ cross-validation (LOOV) approach⁴⁷. This involves systematically removing one observation at a time, using the remaining $n - 1$ points to train the model, and then tests its predictive performance on the excluded point. This process was repeated iteratively for all observations in the dataset, allowing us to assess: (1) the robustness of the models between training and test subsets, and (2) the uncertainty of the estimated coefficients. The R^2 score over the test data was calculated by comparing the predicted values for each test observation with the actual values from the trained model predictions across all test iterations. The R^2 value across all test data for the IJssel winter 2024 event was 0.53, indicating moderate predictive capability. The Meuse summer 2021 event had a stronger median R^2 of 0.81. We calculated the relative interquartile range (IQR) of coefficients across all LOOV iterations, finding that all coefficients had a relative IQR below 0.1, indicating stability.

To evaluate the relative importance of each variable, we standardized both the predictor matrix X and the response variable y using a z-score transformation⁴⁸. This ensures that all variables are on the same scale, allowing for a meaningful comparison of coefficients. Standardized coefficients (Figure 4b and e) show the relative influence of each variable on

the response variable.

Results and discussion

Floodplain plastic deposition increases with flood severity

Plastic deposition on floodplains increases with flood severity, defined by the flood's return period. Higher-magnitude floods lead to increased plastic mass concentrations on floodplains than lower-magnitude events and non-flood conditions (Figure 3). This trend is supported by strong correlations between plastic mass concentrations and both flood return period (T) (Spearman's $\rho = 0.52$, Pearson's $\rho = 0.65$, p-value < 0.05) and river discharge (Spearman's $\rho = 0.76$, Pearson's $\rho = 0.84$, p-value < 0.05). The most severe flood ($T > 100$ years) on the Meuse resulted in the highest plastic mass concentrations, with 11.2 g/m^2 , nearly twice that of non-flood conditions. Similarly, the largest flood event on the IJssel in winter 2024 ($T = 3$ years) led to the highest recorded plastic mass concentrations for that river (3.3 g/m^2), about three times more than during non-flood conditions.

This relationship between flood severity and plastic deposition is similar to trends observed in sediment studies, where higher floodplain deposition rates correspond to increased flood severity^{11,49}. Differences in regression line intercepts between the Meuse and IJssel indicate that the relationship is river-specific, likely reflecting baseline plastic pollution levels (Figure 3). Despite the overall trend showing increased plastic deposition with flood severity, significant variability is noticeable for the Meuse. While plastic deposition generally increases with flood severity, variability in plastic concentrations between the considered events is notable for the Meuse. Some non-flood periods had higher plastic concentrations than the winter 2020 flood, suggesting that factors beyond flood severity, such as legacy plastics or post-flood clean-up efforts, may also influence deposition rates. Furthermore, the relationship between plastic item concentrations and flood return period is less straightforward than that of plastic mass concentrations (Figure S1 in Supporting Information). This

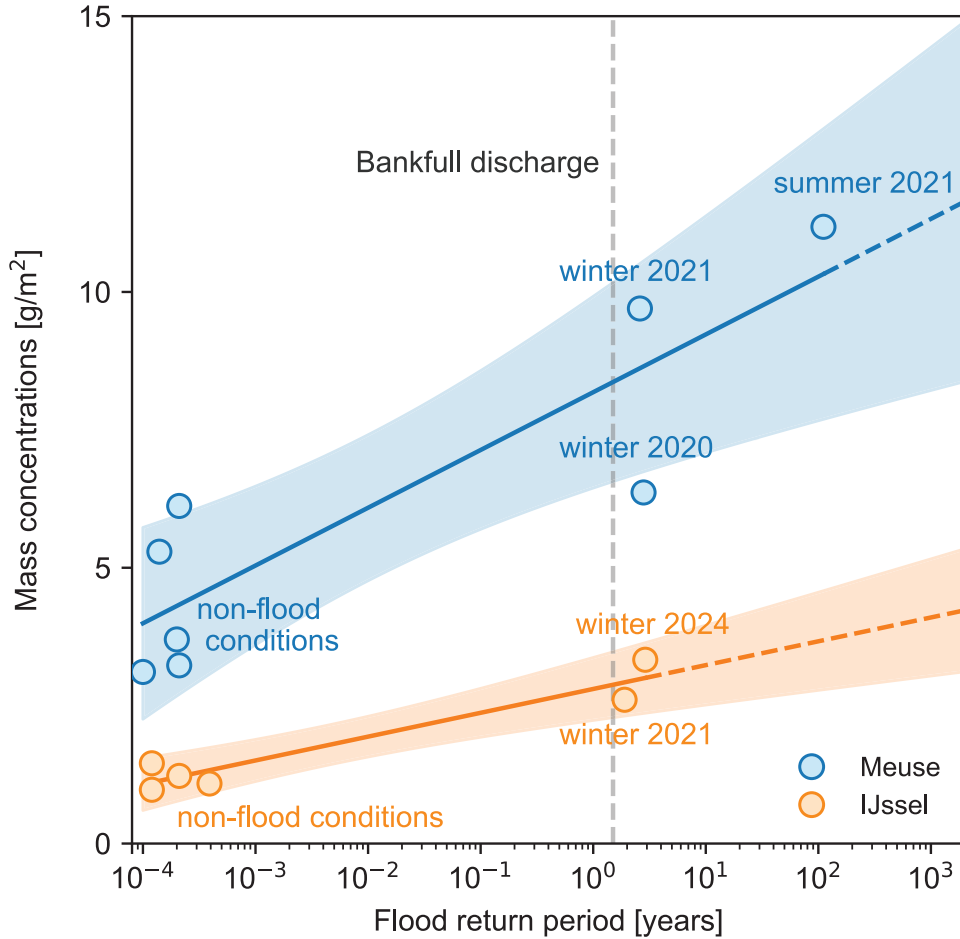


Figure 3: Observed increase in plastic mass concentrations as a function of flood return period. Bankfull discharge is indicated using the 1.5-year return period, consistent with literature for natural rivers that are in equilibrium^{17,18}. The shaded areas represent the 95% confidence interval. The dashed line projects observed trends.

discrepancy may be attributed to fragmentation processes⁵⁰, where item numbers increase without a corresponding mass increase.

The two highest-magnitude floods deposited 4620 tons of plastic along the 240 km of the Dutch Meuse, and 610 tons of plastic along 120 km of the IJssel (Table 3). Plastic storage following floods was two to three times higher than that observed during non-flood conditions. Comparing these storage values with upstream and downstream annual in-river plastic transport reveals that the total plastic mass retained during floods equates to 62–83 years of annual mass transport for the Meuse and 15–41 years for the IJssel (Table 3). These

time-equivalent values indicate how long it would take for the river to transport an equivalent mass of plastic to that found on riverbanks and floodplains. While these values should not be taken as precise indicators of retention times due to inherent uncertainties, they align with evidence of multi-decade-long plastic accumulation on floodplains⁵¹.

Table 3: Plastic storage increases significantly following major floods. Non-flood storage values represent the average from ten events.

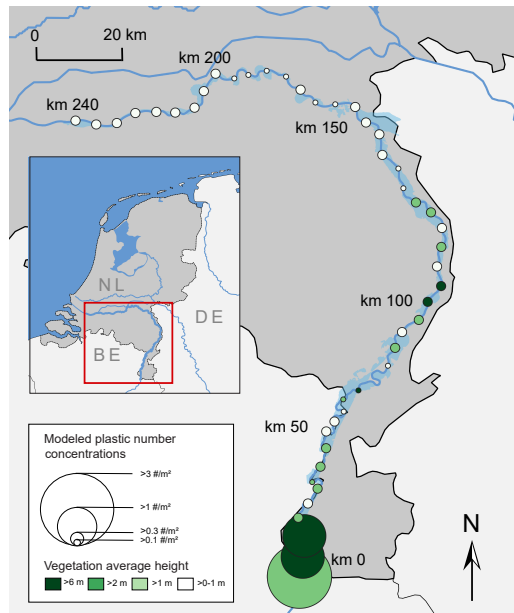
	Annual transport [tons/y]	Storage [tons]		Time-equivalent [y]	
		Flood	Non-flood	Flood	Non-flood
Meuse	56-75	4,620	1,937	62-83	26-35
IJssel	15-41	610	222	15-41	5-15

Driving mechanisms of plastic deposition depend on flood type

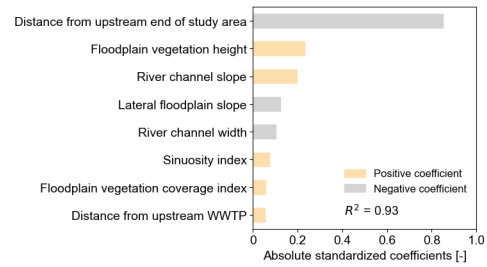
We estimated plastic concentrations with high accuracy for the two highest magnitude floods ($R^2 = 0.93$ for the Meuse summer 2021 flood and $R^2 = 0.83$ for the IJssel winter 2024 flood, Figure 4b and f), using models incorporating eight factors. In the summer 2021 Meuse flood, the primary governing factor was the distance from the upstream end of the study area (Figure 4b). This aligns with reports of extensive damage in the Belgian Meuse catchment, particularly in the Vesdre tributary⁵². Besides source proximity, flood severity was much higher upstream in the Dutch Meuse, ranging from a return period of > 100 years at the most upstream station (km 10) to ~ 10 years at the most downstream station (km 155)³⁴.

We characterize the summer 2021 flood along the Dutch Meuse as following an obstruction-based deposition pattern, where most of the plastic was deposited in floodplain areas that had inundated vegetation (Figure 5a). These high accumulation floodplain zones correspond to areas where river slope was steeper (~ 0.04 m/m) than in the rest of the Dutch Meuse (~ 0.01 m/m) (Figure 4b) and where flow velocities as high as 6 m/s were recorded⁵³. Plastic concentrations depleted rapidly after km 15 (Figure 4a) due to extensive upstream deposition within vegetation. This highlights the role of riparian vegetation in retaining plastic during high-energy flow conditions⁵⁴, and reducing its downstream transport.

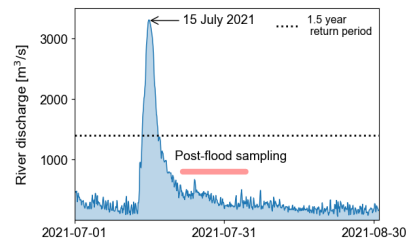
a) Meuse - Spatial distribution



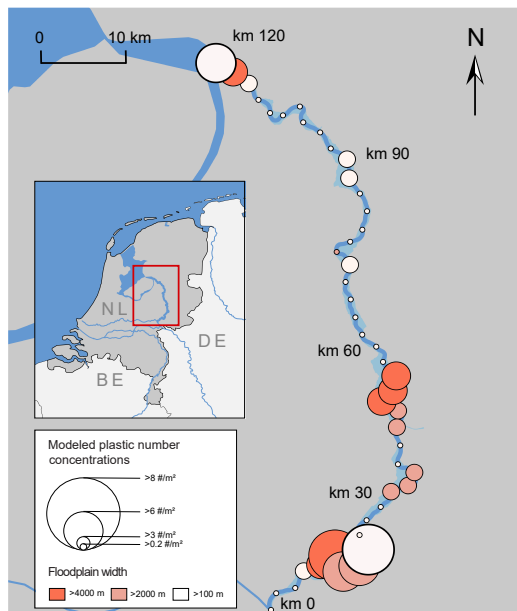
b) Meuse model variables



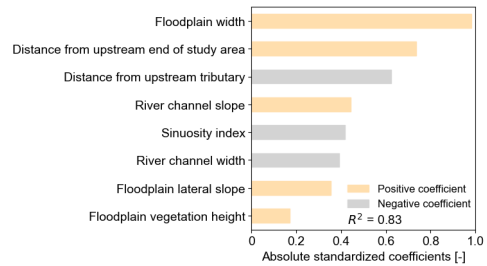
c) Meuse flood discharge record



d) IJssel - Spatial distribution



e) IJssel model variables



f) IJssel flood discharge record

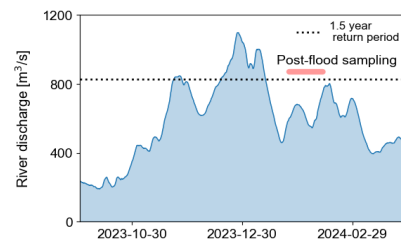


Figure 4: Modeled plastic concentrations along the Meuse (a) and IJssel (d) rivers, showing the impact of key explanatory variables. Concentration values were aggregated in bins of 5 km for the Meuse and 2.5 km for the IJssel. For both floods, eight variables significantly explained plastic deposition (b, e). The hydrological characteristics of the floods differed: the summer 2021 Meuse flood was an extreme event (c), whereas the winter 2024 IJssel flood was a long winter flood event (f).

The winter 2024 IJssel flood showed a different pattern, where floodplain width was found to be the primary factor explaining plastic deposition (Figure 4d). Wider floodplains were linked to higher plastic concentrations, likely due to lower cross-section flow velocities^{37,38}. Proximity to tributaries was also significant factor (Figure 4e), consistent with short plastic transport distances (0.2 - 12 km/day)^{26,51,55}. The winter 2024 event did not cause significant damage to the built environment. However, the recorded increase in plastic concentrations may have resulted from the mobilization of plastics suspended in the water column and/or buried in riverbed sediments. We define this as a low-energy deposition pattern (Figure 5b).

Models' performances for non-flood conditions and low-magnitude floods were lower ($R^2 < 0.5$) (Table S1 in Supporting Information). We found a strong correlation between return period and model performance (Pearson's $\rho = 0.72$, Spearman's $\rho = 0.67$, p-values < 0.05), indicating that as the return period increases, the model's performance improves. During lower-magnitude floods, floodplains were either not activated or only partially so, limiting the influence of floodplain-related variables. Additionally, point-source variables in our model showed no significant correlation with plastic concentrations during low-magnitude floods and non-flood conditions, suggesting these sources were inactive during such events⁵⁶. This aligns with previous findings that most plastic deposition on riverbanks during non-flood conditions could not be attributed to deterministic factors²⁹.

Impact of extreme floods on plastic deposition

The summer 2021 flood deposited 4,620 tons of plastic in the Dutch Meuse floodplains — nearly 30% of the catchment's annual mismanaged plastic waste (15,915 tons/y)⁵⁷. This high deposition is due to the large mass per item (mean: 13.4 g/#), four times higher than that during the IJssel winter 2024 flood (3.3 g/#). This mass per item is also considerably higher than that observed in other river systems globally, such as the Saigon River (3.2 g/#)⁵⁸. Deposition varied significantly, reaching up to 184 g/m² in the most affected area and just 0.4 g/m² in the least affected (Figure S2a in Supporting Information). The extensive

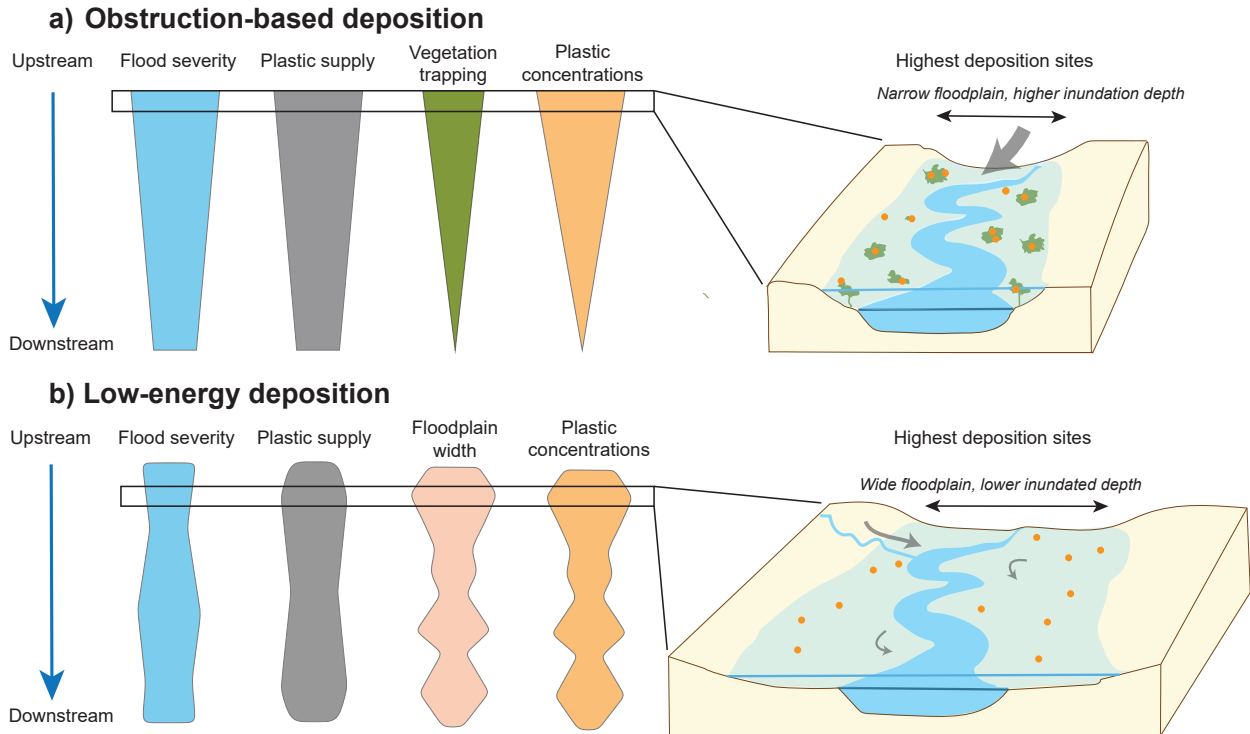


Figure 5: Conceptual representation of plastic deposition patterns along floodplains. a) Obstruction-driven deposition, observed during the summer 2021 Meuse flood. The main plastic supply source (grey arrow) originates from the upstream end of the study domain, with plastics primarily depositing on floodplain zones with inundated trees, deep floodplain water levels and high flow velocities. b) Low-energy deposition observed during the winter 2024 IJssel flood. Plastic supply sources are more diffuse, and greater deposition rates are observed in wide floodplains with reduced cross-section flow velocities. The schematized trends are derived from our observations and forecasting models, as well as literature on flood severity (cf. section ‘Flood severity calculation’.)

deposition observed upstream of the Dutch Meuse was likely driven by extensive damage to the built environment caused by the flood⁵² as well as inputs from Combined Sewer Overflows (CSOs)⁹. The deposited material differed from the typical mismanaged plastic waste and consisted of both waste plastics and non-waste plastics that were mobilized during the flood¹³. The severe impact of this event shows the critical role that extreme floods play in amplifying plastic pollution in aquatic systems well beyond leakage from water management infrastructure. Addressing plastic pollution is not just a matter of waste management but also of flood resilience, as it helps mitigate both physical damage to built environments and

the resulting mobilization of plastics during extreme floods¹⁶.

Our results reveal significant spatial variability in plastic deposition along the river, with an exponential decrease in the Dutch Meuse during the summer 2021 event. We did not sample areas most affected by this event, which were in the Belgian Meuse tributaries. In the Dutch Meuse, plastic and debris followed an uncongested pattern, covering a small portion of the channel^{56,59}. Upstream, tributaries showed semi-congested or congested transport patterns, with debris forming dense surface carpets⁶⁰. This congestion, often mixed with wood and other materials⁶¹, likely influenced the volume and mass of debris deposited on floodplains.

Plastic entry into aquatic systems is expected to rise due to increased global plastic production and consumption⁶², while climate change may lead to more frequent severe floods^{63,64}. This is concerning, as 24% of the global population lives in flood-prone areas⁶⁵. As a result, mobilized plastics during floods are likely to increase. Strengthening flood resilience could mitigate damage to built environments and reduce the influx of new plastic into aquatic systems during extreme events. Additionally, insufficient plastic removal from floodplains may contribute to a growing legacy of plastic pollution on floodplains from past deposition events.

Outlook: towards forecasting of flood-driven plastic deposition

Our study highlights the significant impact of floods on plastic deposition in floodplains. However, current research is limited to two lowland rivers in the Netherlands with relatively low baseline pollution⁶⁶ and focuses on a small number of flood events ($n = 5$). Nevertheless, this represents a larger dataset of flood-related plastic deposition than any previous study, providing unprecedented insight into the role of floods in plastic transport and deposition. Future studies should include a broader range of flood events, river systems, and pollution levels. In-situ sampling during and after floods is crucial but challenging due to accessibility issues, and continuous monitoring of hydrological conditions is necessary for safety and

accessibility.

Literature suggests the existence of multiple flood-transport regimes for debris⁵⁹, each potentially leading to distinct deposition patterns⁶⁷. For instance, flash floods in small systems may result in catchment-wide flushing⁶⁸, a pattern we did not observe in our study. Previous research⁵ reported a decrease in (micro)plastic abundance in riverbed sediments following floods, contrasting with our findings of increased (macro)plastic deposition on floodplains. Hauk et al.⁹ also observed that certain plastic types were preferentially deposited, whereas others were flushed out of the system. These additional patterns show the complexity of plastic transport and retention within river systems during flood events, where both flushing and retention processes can coexist depending on flood dynamics, river morphology, specific river sinks and plastic characteristics.

To effectively reduce plastic accumulation on floodplains, further studies are needed on the spatial distribution to inform reduction measures. Our typologies of floodplain plastic deposition (Figure 5) suggest distinct spatial patterns. Plastics deposited during flood events with obstruction-based deposition clusters around or within floodplain vegetation. In contrast, plastics deposited during low-energy deposition might be distributed in lines parallel to the high water line⁶⁹. Identifying these patterns can help develop targeted, cost-effective interventions. Our model, applicable to other flood events, does not rely on hydrological conditions but requires activated floodplains, as floodplain width and vegetation height are key to explaining deposition patterns.

Acknowledgement

We thank all the colleagues who contributed to the post-flood sampling: Derk van Grootheest, Sjoukje de Lange, Awad Mohammed Ali, Ámbar Pérez-García, Rose Pinto, Silke Tas, Paolo Tasseron, Khoa van le Thi and Miranda Stibora. We also thank all the volunteers from *Schone Rivieren* for their efforts in floodplain plastic monitoring and Winnie de Winter from

Schone Rivieren for sharing the data with us.

Supporting Information Available

The Supporting Information will be made available free of charge upon publication.

Plastic item concentrations increase as a function of flood return period; Modeled plastic concentrations along the upstream-downstream gradient, with key explanatory variables for the Meuse during the summer 2021 flood and the IJssel during the winter 2024 flood; Model formulations, coefficients and performance.

References

- (1) Thompson, R. C.; Courtene-Jones, W.; Boucher, J.; Pahl, S.; Raubenheimer, K.; Koelmans, A. A. Twenty years of microplastics pollution research—what have we learned? *Science* **2024**, *386*, eadl2746.
- (2) Bergmann, M.; Almroth, B. C.; Brander, S. M.; Dey, T.; Green, D. S.; Gundogdu, S.; Krieger, A.; Wagner, M.; Walker, T. R. A global plastic treaty must cap production. *Science* **2022**, *376*, 469–470.
- (3) Bosker, M.; Buringh, E. City seeds: Geography and the origins of the European city system. *Journal of Urban Economics* **2017**, *98*, 139–157.
- (4) Cottom, J. W.; Cook, E.; Velis, C. A. A local-to-global emissions inventory of macroplastic pollution. *Nature* **2024**, *633*, 101–108.
- (5) Hurley, R.; Woodward, J.; Rothwell, J. J. Microplastic contamination of river beds significantly reduced by catchment-wide flooding. *Nature Geoscience* **2018**, *11*, 251–257.

- (6) Mennekes, D.; Mellink, Y. A.; Schreyers, L. J.; van Emmerik, T. H.; Nowack, B. Macroplastic Fate and Transport Modeling: Freshwaters Act as Main Reservoirs. *Environmental Science & Technology Water* **2024**,
- (7) Schreyers, L. J.; van Emmerik, T. H.; Huthoff, F.; Collas, F. P.; Wegman, C.; Vriend, P.; Boon, A.; de Winter, W.; Oswald, S. B.; Schoor, M. M.; Wallerstein, N.; van der Ploeg, M.; Uijlenhoet, R. River plastic transport and storage budget. *Water Research* **2024**, *259*, 121786.
- (8) Grosfeld, J. Macrolitter in Groyne Fields: Short term variability & the influence of natural processes. M.Sc. thesis, Delft University of Technology, 2022.
- (9) Hauk, R.; van Emmerik, T. H.; van der Ploeg, M.; de Winter, W.; Boonstra, M.; Löhr, A. J.; Teuling, A. J. Macroplastic deposition and flushing in the Meuse river following the July 2021 European floods. *Environmental Research Letters* **2023**, *18*, 124025.
- (10) Van Emmerik, T.; Mellink, Y.; Hauk, R.; Waldschläger, K.; Schreyers, L. Rivers as plastic reservoirs. *Frontiers in Water* **2022**, *3*, 212.
- (11) Asselman, N. E.; Middelkoop, H. Temporal variability of contemporary floodplain sedimentation in the Rhine–Meuse delta, The Netherlands. *Earth Surface Processes and Landforms: The Journal of the British Geomorphological Group* **1998**, *23*, 595–609.
- (12) Gurnell, A.; Piégay, H.; Swanson, F.; Gregory, S. Large wood and fluvial processes. *Freshwater Biology* **2002**, *47*, 601–619.
- (13) Valero, D.; Bayón, A.; Franca, M. J. Urban Flood Drifters (UFDs): Onset of movement. *Science of the Total Environment* **2024**, *927*, 171568.
- (14) Van Emmerik, T. H.; Frings, R. M.; Schreyers, L. J.; Hauk, R.; de Lange, S. I.;

- Mellink, Y. A. River plastic transport and deposition amplified by extreme flood. *Nature Water* **2023**, 1–9.
- (15) Tramoy, R.; Gasperi, J.; Dris, R.; Colasse, L.; Fisson, C.; Sananes, S.; Rocher, V.; Tassin, B. Assessment of the Plastic Inputs From the Seine Basin to the Sea Using Statistical and Field Approaches. *Frontiers in Marine Science* **2019**, *6*.
- (16) Van Emmerik, T. H. The impact of floods on plastic pollution. *Global Sustainability* **2024**, 1–13.
- (17) Dury, G.; Hails, J.; Robbie, H. Bankfull discharge and the magnitude frequency series. *Australian Journal of Science* **1963**, *26*, 123–124.
- (18) Leopold, L. B.; Wolman, M. G.; Miller, J. P.; Wohl, E. E. *Fluvial processes in geomorphology*; Courier Dover Publications, 1964; p 544.
- (19) Wohl, E. Bridging the gaps: An overview of wood across time and space in diverse rivers. *Geomorphology* **2017**, *279*, 3–26.
- (20) Wilcock, P. R. Critical shear stress of natural sediments. *Journal of Hydraulic Engineering* **1993**, *119*, 491–505.
- (21) Williams, A.; Simmons, S. The degradation of plastic litter in rivers: implications for beaches. *Journal of Coastal Conservation* **1996**, *2*, 63–72.
- (22) Kawecki, D.; Nowack, B. Polymer-specific modeling of the environmental emissions of seven commodity plastics as macro-and microplastics. *Environmental Science & Technology* **2019**, *53*, 9664–9676.
- (23) Newbound, R.; Powell, D. M.; Whelan, M. Understanding river plastic transport with tracers and GPS. *Nature Reviews Earth & Environment* **2021**, *2*, 591.
- (24) Cesarini, G.; Scalici, M. Riparian vegetation as a trap for plastic litter. *Environmental Pollution* **2022**, *292*, 118410.

- (25) Kuizenga, B.; van Emmerik, T.; Waldschläger, K.; Kooi, M. Will it Float? Rising and Settling Velocities of Common Macroplastic Foils. *Environmental Science & Technology Water* **2021**, *2*, 975–981.
- (26) Lotcheris, R. A.; Schreyers, L.; Bui, T.; Van Le Thi, K.; Nguyen, H.-Q.; Vermeulen, B.; van Emmerik, T. Plastic does not simply flow into the sea: River transport dynamics affected by tides and floating plants. *Environmental Pollution* **2024**, *345*, 123524.
- (27) Van Emmerik, T.; Roebroek, C.; de Winter, W.; Vriend, P.; Boonstra, M.; Hougee, M. Riverbank macrolitter in the Dutch Rhine–Meuse delta. *Environmental Research Letters* **2020**, *15*, 104087.
- (28) De Lange, S. I.; Mellink, Y.; Vriend, P.; Tasseron, P. F.; Begemann, F.; Hauk, R.; Aalderink, H.; Hamers, E.; Jansson, P.; Joosse, N.; Löhr, A. J.; Lotcheris, R.; Schreyers, L.; Vos, V.; van Emmerik, T. H. M. Sample size requirements for riverbank macrolitter characterization. *Frontiers in Water* **2023**, *4*.
- (29) Roebroek, C. T. J.; Hut, R.; Vriend, P.; de Winter, W.; Boonstra, M.; van Emmerik, T. H. M. Disentangling variability in riverbank macrolitter observations. *Environmental Science & Technology* **2021**, *55*, 4932–4942.
- (30) Van Emmerik, T.; de Lange, S.; Frings, R.; Schreyers, L.; Aalderink, H.; Leusink, J.; Begemann, F.; Hamers, E.; Hauk, R.; Janssens, N.; others Hydrology as a driver of floating river plastic transport. *Earth's Future* **2022**, *10*, e2022EF002811.
- (31) Rijkswaterstaat - Ministerie van Infrastructuur en Waterstaat Waterinfo. <https://waterinfo.rws.nl/>, 2024; [Accessed 01-06-2024].
- (32) Raes, D. Frequency analysis of rainfall data. *KU Leuven Inter-University Programme in Water Resources Engineering* **2004**, *42*.

- (33) Van Campenhout, J.; Houbrechts, G.; Peeters, A.; Petit, F. Return period of characteristic discharges from the comparison between partial duration and annual series, application to the Walloon Rivers (Belgium). *Water* **2020**, *12*, 792.
- (34) Slomp, R. *Flooding in the Meuse river basin in the Netherlands - Thursday July 15th - Thursday July 22nd, coping with a summer flood, some first impressions*; 2021.
- (35) Chowdhury, M. K.; Blom, A.; Ylla Arbós, C.; Verbeek, M. C.; Schropp, M. H.; Schielen, R. M. Semicentennial response of a bifurcation region in an engineered river to peak flows and human interventions. *Water Resources Research* **2023**, *59*, e2022WR032741.
- (36) Hastie, T. J. *Statistical models in S*; Routledge, 2017; pp 249–307.
- (37) Savenije, H. H. The width of a bankfull channel; Lacey’s formula explained. *Journal of Hydrology* **2003**, *276*, 176–183.
- (38) Hjulström, F. Transportation of detritus by moving water. Ph.D. thesis, University of Uppsala, 1939.
- (39) Holland, P. G. *Encyclopedia of Hydrology and Lakes*; Springer Netherlands: Dordrecht, 1998; pp 121–121.
- (40) Schreyers, L. J.; van Emmerik, T. H.; Bui, T.-K. L.; van Thi, K. L.; Vermeulen, B.; Nguyen, H.-Q.; Wallerstein, N.; Uijlenhoet, R.; van der Ploeg, M. River plastic transport affected by tidal dynamics. *Hydrology and Earth System Sciences* **2024**, *28*, 589–610.
- (41) Kuizenga, B.; Tasseron, P. F.; Wendt-Potthoff, K.; van Emmerik, T. H. From source to sea: Floating macroplastic transport along the Rhine river. *Frontiers in Environmental Science* **2023**, *11*, 1180872.
- (42) Rijkswaterstaat - Ministerie van Infrastructuur en Waterstaat Ecotopen. <https://>

- waterinfo-extra.rws.nl/monitoring/biologie/ecotopen/, 2024; [Accessed 13-05-2024].
- (43) Actueel Hoogtebestand Nederland (AHN) ATOM Digital Surface Model (DSM) 0,5m and Digital Elevation Model (DEM 0,5m). <https://service.pdok.nl/rws/ahn/atom/index.xml>, 2024; [Accessed 26-02-2024].
- (44) Digitaal Vlaanderen Het Digitaal Hoogtemodel. <https://www.vlaanderen.be/digitaal-vlaanderen/onze-oplossingen/earth-observation-data-science-eodas/het-digitaal-hoogtemodel>, 2024; [Accessed 07-03-2024].
- (45) Stichting Nederlandse WaterSector Watersector Database. <https://watersector.nl/rwzi/map/rwzi>, 2024; [Accessed 06-06-2024].
- (46) Efron, B. *Breakthroughs in statistics: Methodology and distribution*; Springer, 1992; pp 569–593.
- (47) Hastie, T.; Tibshirani, R.; Friedman, J. *The elements of statistical learning: data mining, inference, and prediction*; Springer, 2017; p 764.
- (48) Pedregosa, F. Scikit-learn: Machine learning in python Fabian. *Journal of machine learning research* **2011**, *12*, 2825.
- (49) Jeffries, R.; Darby, S. E.; Sear, D. A. The influence of vegetation and organic debris on flood-plain sediment dynamics: case study of a low-order stream in the New Forest, England. *Geomorphology* **2003**, *51*, 61–80.
- (50) Liro, M.; Zielonka, A.; van Emmerik, T. H. Macroplastic fragmentation in rivers. *Environment International* **2023**, *180*, 108186.
- (51) Tramoy, R.; Gasperi, J.; Colasse, L.; Tassin, B. Transfer dynamic of macroplastics in estuaries — New insights from the Seine estuary: Part 1. Long-term dynamic based on

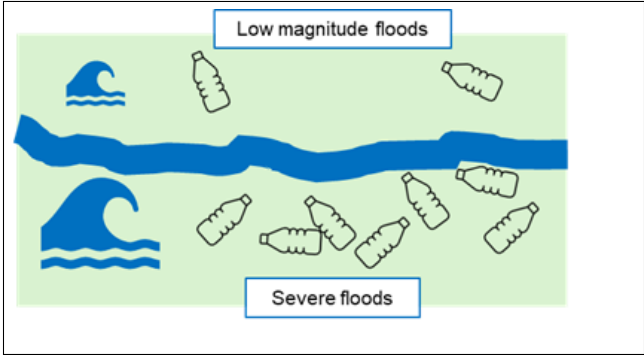
- date-prints on stranded debris. *Marine Pollution Bulletin* **2020**, *152*, 110894, Publisher: Elsevier BV.
- (52) Dewals, B.; Erpicum, S.; Piroton, M.; Archambeau, P. Extreme floods in Belgium. The July 2021 extreme floods in the Belgian part of the Meuse basin. *Hydrolink* **2021**,
- (53) Barneveld, H.; Frings, R.; Mosselman, E.; Venditti, J.; Kleinhans, M.; Blom, A.; Schielen, R.; Toonen, W.; Meijer, D.; Paarlberg, A.; others Extreme River Flood Exposes Latent Erosion Risk From Human Control Measures. 2024; In review.
- (54) Tanaka, N.; Yagisawa, J.; Yasuda, S. Breaking pattern and critical breaking condition of Japanese pine trees on coastal sand dunes in huge tsunami caused by Great East Japan Earthquake. *Natural Hazards* **2013**, *65*, 423–442.
- (55) Hauk, R.; van der Ploeg, M.; Teuling, A. J.; de Winter, W.; van Emmerik, T. H. Plastic transport dynamics revealed through flood induced buttertub spill. *Tomorrow's Rivers* **2024**, *36*, 80.
- (56) Roebroek, C.; Teuling, A. J.; van der Ploeg, M.; González-Fernández, D.; van Emmerik, T. Limited role of discharge in global river plastic transport. 2024; In review.
- (57) Lebreton, L. C.; Van Der Zwet, J.; Damsteeg, J.-W.; Slat, B.; Andrady, A.; Reisser, J. River plastic emissions to the world's oceans. *Nature communications* **2017**, *8*, 1–10.
- (58) Van Emmerik, T.; Kieu-Le, T.-C.; Loozen, M.; van Oeveren, K.; Strady, E.; Bui, X.-T.; Egger, M.; Gasperi, J.; Lebreton, L.; Nguyen, P.-D.; others A methodology to characterize riverine macroplastic emission into the ocean. *Frontiers in Marine Science* **2018**, *5*, 372.
- (59) Ruiz-Villanueva, V.; Mazzorana, B.; Bladé, E.; Bürkli, L.; Iribarren-Anacona, P.; Mao, L.; Nakamura, F.; Ravazzolo, D.; Rickenmann, D.; Sanz-Ramos, M.; others Char-

- acterization of wood-laden flows in rivers. *Earth Surface Processes and Landforms* **2019**, *44*, 1694–1709.
- (60) Erpicum, S.; Poppema, D.; Burghardt, L.; Benet, L.; Klopries, E.-M.; Wuthrich, D.; Dewals, B. Database - Bridge clogging and debris - July 2021 flood. 2024.
- (61) Hoellein, T. J.; Schwenk, B. A.; Kazmierczak, E. M.; Petersen, F. Plastic litter is a part of the carbon cycle in an urban river: Microplastic and macroplastic accumulate with organic matter in floating debris rafts. *Water Environment Research* **2024**, *96*, e11116.
- (62) Borrelle, S. B. et al. Predicted growth in plastic waste exceeds efforts to mitigate plastic pollution. *Science* **2020**, *369*, 1515–1518.
- (63) Slater, L.; Villarini, G.; Archfield, S.; Faulkner, D.; Lamb, R.; Khouakhi, A.; Yin, J. Global changes in 20-year, 50-year, and 100-year river floods. *Geophysical Research Letters* **2021**, *48*, e2020GL091824.
- (64) Gudmundsson, L.; Boulange, J.; Do, H. X.; Gosling, S. N.; Grillakis, M. G.; Koutroulis, A. G.; Leonard, M.; Liu, J.; Müller Schmied, H.; Papadimitriou, L.; others Globally observed trends in mean and extreme river flow attributed to climate change. *Science* **2021**, *371*, 1159–1162.
- (65) Devitt, L.; Neal, J.; Coxon, G.; Savage, J.; Wagener, T. Flood hazard potential reveals global floodplain settlement patterns. *Nature Communications* **2023**, *14*, 2801.
- (66) Van Calcar, C. J.; van Emmerik, T. H. Abundance of plastic debris across European and Asian rivers. *Environmental Research Letters* **2019**, *14*, 124051.
- (67) Church, M.; Jakob, M. What is a debris flood? *Water Resources Research* **2020**, *56*, e2020WR027144.
- (68) Pierdomenico, M.; Ridente, D.; Casalbore, D.; Di Bella, L.; Milli, S.; Chiocci, F. L.

Plastic burial by flash-flood deposits in a prodelta environment (Gulf of Patti, Southern Tyrrhenian Sea). *Marine Pollution Bulletin* **2022**, *181*, 113819.

- (69) Tasseron, P. F.; van Emmerik, T. H.; de Winter, W.; Vriend, P.; van der Ploeg, M. Riverbank plastic distributions and how to sample them. *Microplastics and Nanoplastics* **2024**, *4*, 22.

TOC Graphic



Supporting Information for ‘Flood type drives river-scale plastic deposition’

Louise J. Schreyers,^{*,†} Rahel Hauk,[†] Nicholas Wallerstein,[†] Adriaan J. Teuling,[†]
Remko Uijlenhoet,^{†,‡} Martine van der Ploeg,[†] and Tim H.M. van Emmerik[†]

[†]*Hydrology and Environmental Hydraulics Group, Wageningen University, Wageningen*

[‡]*Department of Water Management, Delft University of Technology, Delft*

E-mail: *l.schreyers@gmail.com

References

- (1) Dury, G.; Hails, J.; Robbie, H. Bankfull discharge and the magnitude frequency series. *Australian Journal of Science* **1963**, *26*, 123–124.
- (2) Leopold, L. B.; Wolman, M. G.; Miller, J. P.; Wohl, E. E. *Fluvial processes in geomorphology*; Courier Dover Publications, 1964; p 544.

Table S1: Model formulations, coefficients and performance. Coefficients marked with an asterisk (*) indicate an exponential transformation. Different formulations for the same event are grouped under the same model number, with variations indicated by the letters (e.g., model 1.a and 1.b represent different formulations for event 1).

Model	Calibrated dataset	Floodplain characteristics				River channel characteristics			Point sources			R ² (AIC)
		Width	Vegetation height	Vegetation coverage index	Lateral slope	Sinuosity	Width	Slope	Distance from upstream end of study area	Distance from upstream WWTP	Distance from upstream tributary	
1.a	Meuse summer 2021			$3.6 \cdot 10^{-2}$ (*)	$2.6 \cdot 10^{-2}$		$3.5 \cdot 10^{-4}$	$2.7 \cdot 10^0$				0.92 (-75)
1.b	Meuse summer 2021	$-4.5 \cdot 10^{-4}$	$1.8 \cdot 10^{-1}$	$5.4 \cdot 10^{-1}$	$1.1 \cdot 10^{-2}$	$-1.5 \cdot 10^0$	$-2.8 \cdot 10^{-3}$	$9.0 \cdot 10^1$	$-2.0 \cdot 10^{-5}$	$4.0 \cdot 10^{-5}$	$4.0 \cdot 10^{-5}$	0.73 (-19)
1.c	Meuse summer 2021	$-7.0 \cdot 10^{-5}$	$1.4 \cdot 10^{-1}$	$-1.6 \cdot 10^{-1}$	$3.4 \cdot 10^{-2}$	$1.2 \cdot 10^0$	$-3.5 \cdot 10^{-3}$	$-2.2 \cdot 10^1$	$1.0 \cdot 10^{-5}$	$-1.0 \cdot 10^{-5}$	$-1.0 \cdot 10^{-5}$	0.93 (-72)
1.d	Meuse summer 2021		$1.2 \cdot 10^{-1}$	$-7.9 \cdot 10^{-2}$	$3.1 \cdot 10^{-2}$	$7.6 \cdot 10^{-1}$	$-2.8 \cdot 10^{-3}$	$-1.3 \cdot 10^1$				0.92 (-76)
1.e	Meuse summer 2021		$1.1 \cdot 10^{-1}$		$2.8 \cdot 10^{-2}$	$6.3 \cdot 10^{-1}$	$-2.5 \cdot 10^{-3}$	$-1.3 \cdot 10^1$				0.92 (-78)
1.f	Meuse summer 2021		$1.0 \cdot 10^{-1}$		$4.0 \cdot 10^{-2}$		$3.3 \cdot 10^{-4}$	$1.0 \cdot 10^0$				0.92 (-76)
1.g	Meuse summer 2021		$1.9 \cdot 10^{-1}$									0.85 (-59)
1.h	Meuse summer 2021	$-3.4 \cdot 10^{-4}$	$1.7 \cdot 10^{-1}$	$4.2 \cdot 10^{-1}$	$2.7 \cdot 10^{-2}$	$-8.8 \cdot 10^{-1}$	$1.7 \cdot 10^{-3}$	$5.4 \cdot 10^1$	$-2.0 \cdot 10^{-5}$	$3.0 \cdot 10^{-5}$	$3.0 \cdot 10^{-5}$	0.72 (-19)
1.i	Meuse summer 2021		$1.4 \cdot 10^{-1}$	$-1.4 \cdot 10^{-1}$	$3.7 \cdot 10^{-2}$	$1.0 \cdot 10^0$	$-3.2 \cdot 10^{-3}$	$-2.5 \cdot 10^1$	$1.0 \cdot 10^{-5}$	$-1.0 \cdot 10^{-5}$	$-1.0 \cdot 10^{-5}$	0.93 (-74)
1.j	Meuse summer 2021		$1.3 \cdot 10^{-1}$	$-8.1 \cdot 10^{-2}$	$3.2 \cdot 10^{-2}$	$7.8 \cdot 10^{-1}$	$-3.1 \cdot 10^{-3}$	$-1.8 \cdot 10^1$	$1.0 \cdot 10^{-5}$	$1.0 \cdot 10^{-5}$	$1.0 \cdot 10^{-5}$	0.93 (-75)
2.a	Meuse winter 2021	$2.6 \cdot 10^{-6}$	$1.8 \cdot 10^{-1}$	$6.9 \cdot 10^{-2}$	$-3.7 \cdot 10^{-2}$	$-2.1 \cdot 10^{-1}$	$5.3 \cdot 10^{-3}$	$7.3 \cdot 10^1$	$5.5 \cdot 10^{-6}$	$-1.1 \cdot 10^{-5}$	$-1.1 \cdot 10^{-5}$	0.47 (-43)
3.a	Meuse winter 2020	$-1.4 \cdot 10^{-4}$	$4.0 \cdot 10^{-3}$	$1.1 \cdot 10^{-1}$	$6.7 \cdot 10^{-2}$	$2.4 \cdot 10^0$	$-8.4 \cdot 10^{-3}$	$-3.3 \cdot 10^1$	$-8.1 \cdot 10^{-6}$	$3.9 \cdot 10^{-5}$	$3.9 \cdot 10^{-5}$	0.43 (-13)
4.a	Meuse fall 2018	$-1.1 \cdot 10^{-5}$	$3.5 \cdot 10^{-3}$	$-3.8 \cdot 10^{-3}$	$9.0 \cdot 10^{-4}$	$-5.0 \cdot 10^{-3}$	$-4.8 \cdot 10^{-4}$	$3.7 \cdot 10^0$	$6.0 \cdot 10^{-7}$	$5.6 \cdot 10^{-6}$	$-1.4 \cdot 10^{-6}$	0.24 (-127)
5.a	Meuse fall 2019	$2.5 \cdot 10^{-5}$	$-1.7 \cdot 10^{-2}$	$-4.3 \cdot 10^{-2}$	$2.0 \cdot 10^{-2}$	$1.8 \cdot 10^{-1}$	$2.2 \cdot 10^{-4}$	$-3.2 \cdot 10^0$	$-1.2 \cdot 10^{-6}$	$-8.0 \cdot 10^{-7}$	$7.1 \cdot 10^{-6}$	0.23 (-151)
6.a	Meuse fall 2020	$-2.6 \cdot 10^{-5}$	$7.7 \cdot 10^{-2}$	$-7.2 \cdot 10^{-2}$	$-1.0 \cdot 10^{-2}$	$6.3 \cdot 10^{-2}$	$4.4 \cdot 10^{-3}$	$5.8 \cdot 10^1$	$-2.7 \cdot 10^{-6}$	$-1.5 \cdot 10^{-6}$	$-2.0 \cdot 10^{-7}$	0.26 (-35)
7.a	Meuse fall 2021	$2.0 \cdot 10^{-7}$	$-1.5 \cdot 10^{-2}$	$8.9 \cdot 10^{-3}$	$1.9 \cdot 10^{-3}$	$3.5 \cdot 10^{-1}$	$-2.7 \cdot 10^{-4}$	$-4.4 \cdot 10^0$	$-1.4 \cdot 10^{-6}$	$1.9 \cdot 10^{-6}$	$-2.0 \cdot 10^{-7}$	0.34 (-279)
9.a	Meuse fall 2022	$6.7 \cdot 10^{-6}$	$-8.2 \cdot 10^{-3}$	$6.4 \cdot 10^{-3}$	$6.6 \cdot 10^{-3}$	$-5.5 \cdot 10^{-2}$	$1.1 \cdot 10^{-3}$	$-5.4 \cdot 10^0$	$-8.0 \cdot 10^{-7}$	$2.0 \cdot 10^{-6}$	$-9.0 \cdot 10^{-7}$	0.21 (-265)
10.a	IJssel winter 2024	$2.7 \cdot 10^{-3}$	$1.5 \cdot 10^0$	$2.2 \cdot 10^{-1}$	$3.1 \cdot 10^{-1}$	$-1.5 \cdot 10^1$	$-4.7 \cdot 10^{-2}$	$1.6 \cdot 10^3$	$2.0 \cdot 10^{-6}$	$2.0 \cdot 10^{-6}$	$-1.5 \cdot 10^{-4}$	0.83 (57)
10.b	IJssel winter 2024	$2.6 \cdot 10^{-3}$	$1.9 \cdot 10^0$	$3.2 \cdot 10^{-1}$	$2.3 \cdot 10^{-1}$	$-1.3 \cdot 10^1$	$-3.2 \cdot 10^{-2}$	$9.5 \cdot 10^2$	$5.8 \cdot 10^{-5}$	$-1.8 \cdot 10^{-5}$	$6.6 \cdot 10^0$ (*)	0.80 (63)
10.c	IJssel winter 2024	$2.7 \cdot 10^{-3}$	$1.7 \cdot 10^0$		$3.2 \cdot 10^{-1}$	$-1.5 \cdot 10^1$	$-4.6 \cdot 10^{-2}$	$1.6 \cdot 10^3$	$9.6 \cdot 10^{-5}$	$-1.5 \cdot 10^{-4}$	$-1.5 \cdot 10^{-4}$	0.83 (53)
11.a	IJssel winter 2021	$2.9 \cdot 10^{-5}$	$-9.8 \cdot 10^{-2}$	$1.1 \cdot 10^{-1}$	$4.6 \cdot 10^{-3}$	$-1.3 \cdot 10^{-1}$	$2.5 \cdot 10^{-3}$	$9.6 \cdot 10^0$	$-5.9 \cdot 10^{-6}$	$-1.3 \cdot 10^{-6}$	$2.0 \cdot 10^{-6}$	0.24 (-183)
12.a	IJssel fall 2020	$-1.4 \cdot 10^{-5}$	$1.9 \cdot 10^{-2}$	$-4.1 \cdot 10^{-2}$	$1.0 \cdot 10^{-3}$	$1.7 \cdot 10^{-1}$	$-1.2 \cdot 10^{-3}$	$1.1 \cdot 10^1$	$7.0 \cdot 10^{-7}$	$-1.4 \cdot 10^{-6}$	$-1.4 \cdot 10^{-6}$	0.37 (-115)
13.a	IJssel fall 2021	$-4.4 \cdot 10^{-6}$	$-3.0 \cdot 10^{-3}$	$3.0 \cdot 10^{-3}$	$2.1 \cdot 10^{-3}$	$-5.9 \cdot 10^{-3}$	$8.3 \cdot 10^{-5}$	$1.1 \cdot 10^0$	$6.0 \cdot 10^{-7}$	$-7.7 \cdot 10^{-9}$	$-1.2 \cdot 10^{-6}$	0.26 (-357)
14.a	IJssel fall 2022	$4.7 \cdot 10^{-6}$	$3.4 \cdot 10^{-2}$	$-5.5 \cdot 10^{-2}$	$2.0 \cdot 10^{-2}$	$1.2 \cdot 10^0$	$2.0 \cdot 10^{-3}$	$-3.7 \cdot 10^1$	$-7.0 \cdot 10^{-7}$	$2.4 \cdot 10^{-6}$	$4.0 \cdot 10^{-7}$	0.30 (-183)
15.a	IJssel fall 2023	$-9.0 \cdot 10^{-7}$	$1.6 \cdot 10^{-2}$	$-1.5 \cdot 10^{-2}$	$7.7 \cdot 10^{-3}$	$-1.5 \cdot 10^{-2}$	$5.1 \cdot 10^{-4}$	$-2.3 \cdot 10^0$	$-3.0 \cdot 10^{-7}$	$-3.0 \cdot 10^{-7}$	$3.0 \cdot 10^{-7}$	0.43 (-235)

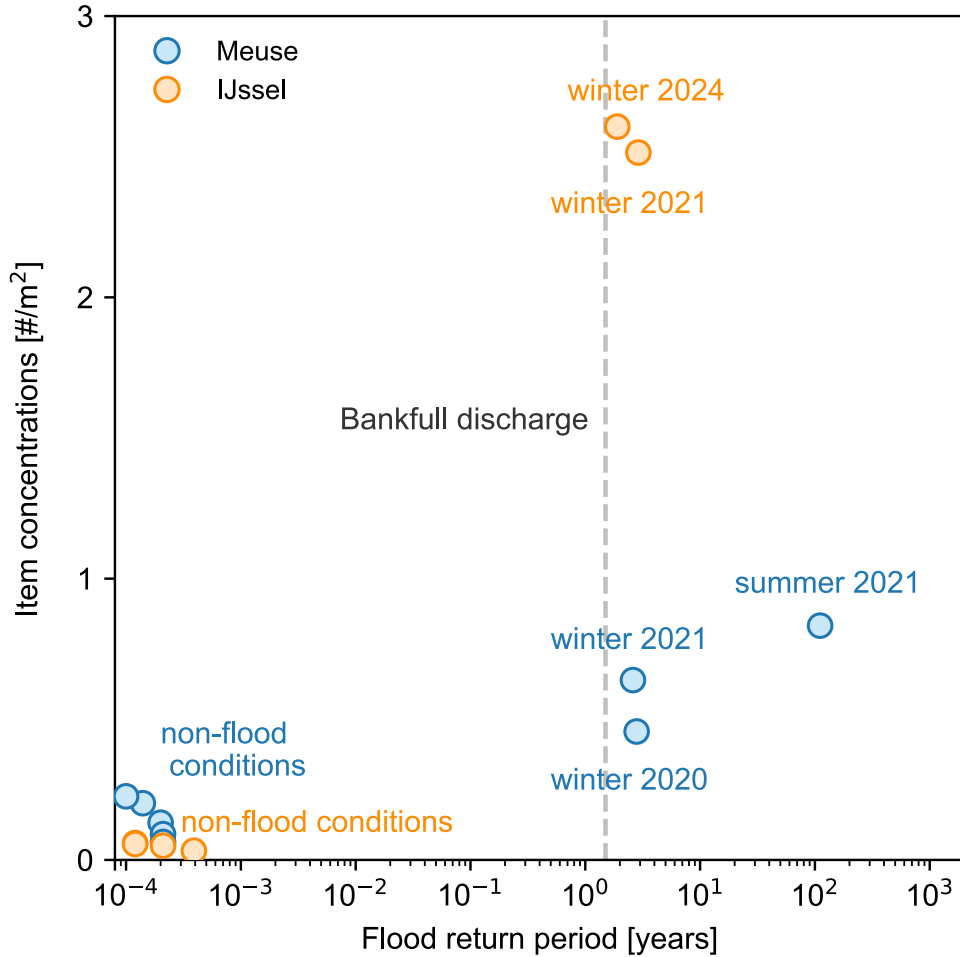
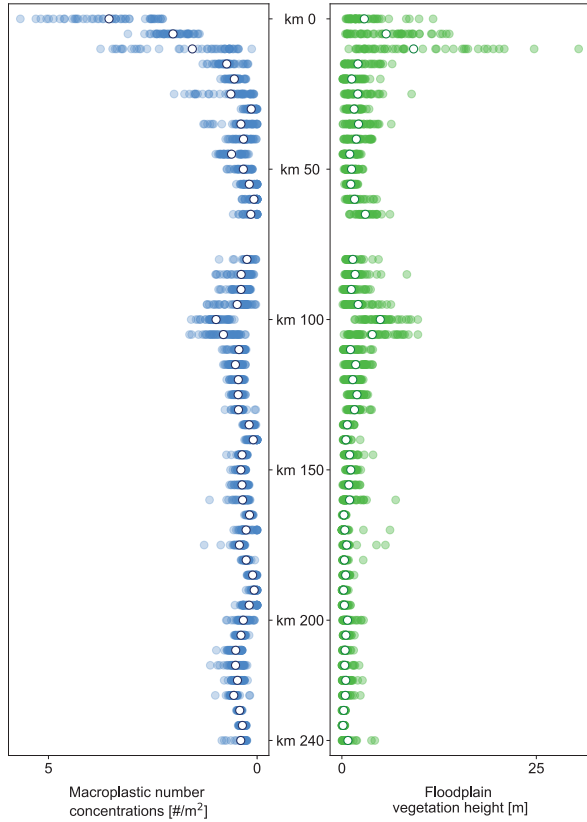


Figure S1: Plastic item concentrations increase as a function of flood return period. A steeper increase is noticeable for the IJssel compared to the Meuse, suggesting that the IJssel experiences higher rates of fragmentation and/or mobilization of sources containing numerous small plastic items as a result of floods. The bankfull discharge is indicated for the 1.5-year return period, consistent with established literature on bankfull discharge in natural rivers^{1,2}.

a) Meuse - summer 2021 flood



b) IJssel - winter 2024 flood

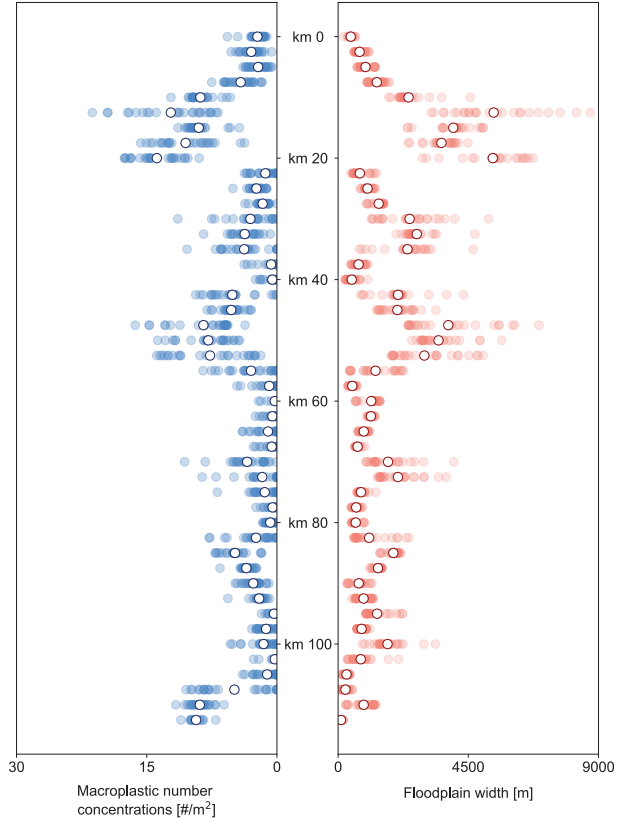


Figure S2: Modeled plastic concentrations along the upstream-downstream gradient, with key explanatory variables for the Meuse during the summer 2021 flood (a) and the IJssel during the winter 2024 flood (b). All values were binned at 5-km resolution for the Meuse and 2.5 km resolution for the IJssel. White dots represent mean values, while colored dots show individual data points.